PRAMANA — journal of physics

Vol. 79, No. 2
August 2012
pp. 287–297

Analytical model of transient temperature and thermal stress in continuous wave double-end-pumped laser rod: Thermal stress minimization study

KHALID S SHIBIB*, MAYADA M TAHIR and HAQI I QATTA
Department of Laser and Optoelectronics Engineering, University of Technology, Baghdad, Iraq
*Corresponding author. E-mail: assprofkh@yahoo.com

MS received 29 September 2011; revised 14 January 2012; accepted 8 February 2012

Abstract. A time-dependent analytical thermal model of the temperature and the corresponding induced thermal stresses in continuous wave double-end-pumped laser rod are derived from the first principle using the integral transform method. The aim of the paper is to study the effect of increasing the pumping powers while the laser crystals are still in the safe zone (i.e. far away from failure stress) and to suitably choose a crystal that achieves this task. The result of this work is compared with a well-verified finite element solution and a good agreement has been found. Some conclusions are obtained: Tm:YAP crystal, which has high thermal conductivity, low expansion coefficient, low absorption coefficient, low thermal factor and low product of $\gamma E/(1-\upsilon)$, is the best choice to reduce induced stress although it is responded and brought to thermal equilibrium faster than the other types of crystal usually used in the end-pumped solid-state laser.

Keywords. Integral transform method; double end-pumped; laser rod; thermal stress.

PACS Nos 44.05.e; 42.55.xi

1. Introduction

Diode-end-pumped solid-state lasers are widely used because of their high compatibility, high efficiency, high output power, good stability and good beam quality. The most determinate factor that limits the increase of their output power is the part of the absorbed power that converts to heat. It may cause thermal stress, stress birefringence and thermal lens effect which may degrade the optical properties of the laser medium, reduce the laser output and beam quality and at excessive thermal stress, it may lead to medium break [1,2].

The reduction of thermal effects which causes a temperature gradient across the laser medium is an important factor in designing high-average-power systems. In order to reduce heat effects, many procedures were followed [3–6]. The most noticeable one is to use a double-end pumping where the pumping power is divided over two ends of the laser

DOI: 10.1007/s12043-012-0295-4; ***e*Publication: 23 June 2012**

crystal which allows an increase in the output power. In this procedure, the thermal load is divided over the two ends of the laser crystal which may extend the possible pumping power before failure stress can be reached.

One of the most valuable methods for designing the laser system is the use of mathematical models. A time-dependent analytical thermal model of the temperature and the corresponding induced thermal stresses in continuous wave double-end-pumped laser rods is derived from its first principle using integral transform method. To the best of our knowledge, this is the first time that the integral transform method has been used to predict the transient temperature distribution in the double-end-pumped laser rod in solid-state laser. The aim of the paper is to study the effect of the increase in pumping powers when the laser crystals are still in the safe zone (i.e. far away from failure stress) and to suitably choose a crystal that achieves this task.

2. Theory

2.1 *Thermal analysis*

The axis-symmetry heat equation is used to simulate the energy transfer through the laser rod that pumped from both of its ends. The equation can be written as [7]

$$\frac{\partial^2 T}{\partial r^2} + \frac{1}{r}\frac{\partial T}{\partial r} + \frac{\partial^2 T}{\partial z^2} + \frac{Q}{k} = \frac{\rho c}{k}\frac{\partial T}{\partial t} \tag{1}$$

ρ, c, k are respectively the density (kg/m^3), specific heat (J/kg·K) and thermal conductivity (W/m·K), r and z are the radial and longitudinal coordinates (m), Q is the heat generation (W/m^3), T is the temperature (K).

The boundary conditions are (see figure 1):

$$k\frac{\partial T}{\partial r} = h(T_\infty - T), \qquad \text{at } r = r_2, \tag{1a}$$

$$\frac{\partial T}{\partial z} = 0, \qquad \text{at } z = 0,\ z = \ell, \tag{1b}$$

$$\frac{\partial T}{\partial r} = 0, \qquad \text{at } r = 0. \tag{1c}$$

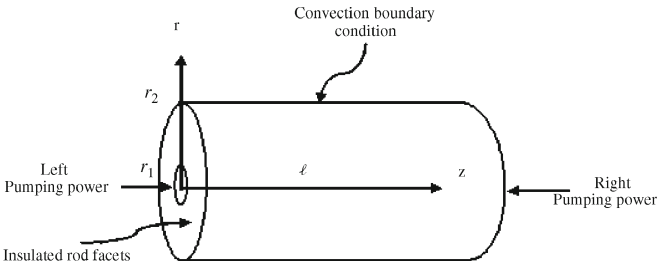

Figure 1. The studied domain and boundary conditions of the laser rod.

Here h is the convection heat transfer coefficient (W/m^2·K), ℓ is the length of the rod (m), r_2 is the outside rod radius. The initial and environmental temperatures (T_∞) are equal to 25°C. The part of the absorbed power from both laser ends that converts to heat acts as a heat source and for top hat beam it can be written as [8]

$$Q_l = \begin{cases} \dfrac{\eta\alpha P_\mathrm{l}\exp(-\alpha z)}{\pi r_1^2\left[1-\exp(-\alpha\ell)\right]}, & 0 \le r \le r_1, t \ge 0 \\ 0, & r_1 \le r \le r_2, t \ge 0 \\ 0, & t < 0 \end{cases} \tag{2}$$

$$Q_r = \begin{cases} \dfrac{\eta\alpha P_\mathrm{r}\exp(-\alpha(\ell - z))}{\pi r_1^2\left[1-\exp(-\alpha\ell)\right]}, & 0 \le r \le r_1, t \ge 0 \\ 0, & r_1 \le r \le r_2, t \ge 0 \\ 0, & t < 0 \end{cases} \tag{2a}$$

r_1 is the pumping radius (m), η is a unitless thermal factor, α is the absorption coefficient (m^{-1}), P_l, P_r are the pumping power in watts from left and right. The integral transform method discussed by Özisik [7], is followed here where the final form of the solution is

$$\theta = \sum_{m=1}^{\infty}\sum_{p=1}^{\infty}\frac{R_0(\beta_m, r)Z(\eta_p, z)}{N(\beta_m)N(\eta_p)}\exp\left(-\frac{k}{\rho c}\left(\beta_m^2+\eta_p^2\right)t\right) \times\left[\frac{1}{\rho c}\int_{t'=0}^{t}\exp\left(\frac{k}{\rho c}\left(\beta_m^2+\eta_p^2\right)t'\right)\cdot\vec{\vec{g}}(\beta_m,\eta_p,t')\mathrm{d}t'\right]. \tag{3}$$

Here

$$\vec{\vec{g}}(\beta_m,\eta_p,t') = \int_{z'=0}^{\ell}\int_{r'=0}^{r_1} r' R_0(\beta_m, r')\cdot Z(\eta_p, z')\cdot g(t')\mathrm{d}r'\mathrm{d}z'. \tag{3a}$$

Also

$$R_0(\beta_m, r) = J_0(\beta_m r), \tag{3b}$$

$$\frac{1}{N(\beta_m)} = \frac{1}{N_m} = \frac{2k^2\beta_m^2}{r_2^2 J_0\left(\beta_m r_2\right)\left(h^2+k^2\beta_m^2\right)}, \tag{3c}$$

$$Z(\eta_p, z) = \cos(\eta_p z). \tag{3d}$$

For convection boundary condition, the roots can be obtained from

$$hJ_0(\beta_m r_2) - k\beta_m J_1(\beta_m r_2) = 0. \tag{4a}$$

Also for insulated rod facets

$$\frac{1}{N(\eta_p)} = \frac{1}{N_p} = \begin{bmatrix} \dfrac{2}{\ell}, & \text{for } \eta_p \ne 0 \\ \dfrac{1}{\ell}, & \text{for } \eta_p = 0 \end{bmatrix}, \tag{4b}$$

where the roots η_p are obtained from

$$\sin(\eta_p \ell) = 0. \tag{4c}$$

The roots included $\eta_p = 0$ (i.e. insulated boundary at the facets of the rod). As shown in eq. (4b), then eq. (3) becomes

$$\begin{aligned}\theta = T - T_\infty = &\sum_{m=1}^{\infty} \frac{2J_0(\beta_m r)}{\rho c N_m \ell} \exp\left(-\frac{k}{\rho c}\beta_m^2 t\right)\left[\int_{\tau=0}^{\tau} \exp\left(\frac{k}{\rho c}\beta_m^2 \tau\right) g_m(\tau)\mathrm{d}\tau\right] \\ &+ \sum_{m=1}^{\infty}\sum_{p=1}^{\infty} \frac{2J_0(\beta_m r)\cos(\eta_p z)}{\rho c N_m \ell} \exp\left(-\frac{k}{\rho c}\left(\beta_m^2 + \eta_p^2\right) t\right) \\ &\times \left[\int_{\tau=0}^{\tau} \exp\left(\frac{k}{\rho c}\left(\beta_m^2 + \eta_p^2\right)\tau\right)\ g_{mp}(\tau)\mathrm{d}\tau\right],\end{aligned} \tag{5}$$

where

$$g_m(\tau) = \int_0^{\ell}\int_0^{r_1} \frac{\eta\alpha P_{1,\mathrm{r}}}{\pi r_1^2 k} \exp(-\alpha z) J_0(\beta_m r) r\ \mathrm{d}r\ \mathrm{d}z \tag{5a}$$

$$g_{mp}(\tau) = \int_0^{\ell}\int_0^{r_1} \frac{\eta\alpha P_{1,\mathrm{r}}}{\pi r_1^2 k} J_0(\beta_m r) \exp(-\alpha z)\cos(\eta_m z) r\ \mathrm{d}r\ \mathrm{d}z. \tag{5b}$$

At a time less than or equal to the time necessary to reach thermal equilibrium, the transform of time (τ) is equal to t in eq. (5). Carrying out the integrations in eqs (5a), (5b) and in eq. (5), then the transient solution can be obtained starting from the rest. Also the time necessary to reach thermal equilibrium can be obtained as the difference between steady-state temperature and the temperature for certain location in the laser rod reduced below a certain value. A general acceptable tolerance is that the current temperature tends towards 99.9% from that of the steady-state temperature. The point where the maximum temperature is reached in the rod, which is proved to occur at the very ends of the laser rod, is the expected tested location since it takes more time to stabilize. Then for $t \le t_s$,

$$\begin{aligned}\theta\ =\ T - T_\infty = &\sum_{m=1}^{\infty} \frac{2\eta P_{1,\mathrm{r}} J_0(\beta_m r) J_1(\beta_m r_1)}{\pi r_1 k N_m \ell \beta_m^3}\left[1 - \exp\left(-\frac{k}{\rho c}\beta_m^2 t\right)\right] \\ &+ \sum_{m=1}^{\infty}\sum_{p=1}^{\infty} \frac{2\eta\alpha^2 P_{1,\mathrm{r}} J_1(\beta_m r_1) J_0(\beta_m r)\cos(\eta_p z)[1 + \cos(\eta_p \ell)]}{\pi r_1 \beta_m k N_m \ell(\beta_m^2 + \eta_p^2)(\alpha^2 + \eta_p^2)} \\ &\times \left[1 - \exp\left(-\frac{k}{\rho c}\left(\beta_m^2 + \eta_p^2\right) t\right)\right].\end{aligned} \tag{6}$$

The steady-state solution can be obtained by setting time equal to infinity where the term that contains time in eq. (6) is vanished, then the solution for steady-state temperature can be written as

$$\begin{aligned}\theta\ =\ T - T_\infty = &\sum_{m=1}^{\infty} \frac{2\eta P_{1,\mathrm{r}} J_0(\beta_m r) J_1(\beta_m r_1)}{\pi r_1 k N_m \ell \beta_m^3} \\ &+ \sum_{m=1}^{\infty}\sum_{p=1}^{\infty} \frac{2\eta\alpha^2 P_{1,\mathrm{r}} J_1(\beta_m r_1) J_0(\beta_m r)\cos(\eta_p z)[1 + \cos(\eta_p \ell)]}{\pi r_1 \beta_m k N_m \ell(\beta_m^2 + \eta_p^2)(\alpha^2 + \eta_p^2)}.\end{aligned} \tag{7}$$

Equation (7) stands for the thermal equilibrium case where a comparison between the transient and steady-state temperatures could be made to simulate the steady-state condition.

2.2 *Stress analysis*

Although different methods have been used to predict failure stress, the maximum tensile hoop stress is proved to model the fracture in laser rod very well [9]. The hotter central portion of the laser rod is compressed by the cooler outer zone which generates compressive stress within the central portion of the rod while a tensile hoop stress is generated in the cooler outer portion. Since the compressive fracture strength is 5–6 times higher than tensile strength for crystal material, it is generally admitted that fracture occurs when the maximum tensile hoop (tangential) stress anywhere in the rod exceeds its yielding tensile stress [9]. A general acceptable value for fracture tensile strength of Nd:YAG material, as suggested by [10], is equal to approximately 138 MPa.

Assume that the rod reaches its thermal stress equilibrium at the end of each time step, then the hoop stress can be written as [11,12]

$$\sigma_\theta = \frac{\gamma E}{(1-\upsilon)}\left[\frac{1}{r_2^2}\int_0^{r_2}\theta r\ \mathrm{d}r + \frac{1}{r^2}\int_0^{r}\theta r\ \mathrm{d}r - \theta\right], \tag{8}$$

where σ_θ is the hoop stress (MPa), E is the modulus of elasticity (MPa), υ is the Poisson ratio and γ is the thermal expansion coefficient (1/K). From eq. (8), it is clear that the hoop stress is reaching its maximum value at the facets of the rod and by assuming the pump power to be equally divided over its two ends, one can obtain the maximum hoop stress by setting z equal to zero and the location and maximum magnitude of the hoop stress through the radial distance can be indicated by obtaining the stress distribution through the face of the rod. Carrying out the integration in eq. (8) and simplifying the hoop stress history before and when reaching thermal equilibrium (i.e. $t \le t_s$) can be written as

$$\begin{aligned}\sigma_\theta = {} & \frac{\gamma E}{(1-\upsilon)}\left[\sum_{m=1}^{\infty}\frac{2\eta P_{l,r} J_1(\beta_m r_1) B}{\pi r_1 k N_m \ell \beta_m^3}\left[1-\exp\left(-\frac{k}{\rho c}\beta_m^2 t\right)\right]\right. \\ & + \sum_{m=1}^{\infty}\sum_{p=1}^{\infty}\frac{2\eta\alpha^2 P_{l,r} J_1(\beta_m r_1) B\cos(\eta_p z)[1+\cos(\eta_p \ell)]}{\pi r_1 \beta_m k N_m \ell(\beta_m^2+\eta_p^2)(\alpha^2+\eta_p^2)} \\ & \left.\times\left[1-\exp\left(-\frac{k}{\rho c}(\beta_m^2+\eta_p^2)t\right)\right]\right]\end{aligned} \tag{9}$$

where

$$B = \frac{J_1(\beta_m r_2)}{\beta_m r_2} + \frac{J_1(\beta_m r)}{\beta_m r} - J_0(\beta_m r).$$

3. Validation

The result of this work is compared with a well-verified finite element solution of the steady-state double-end-pumped Nd:YAG laser rod previously published in [2] where an

Nd:YAG laser rod is pumped by a top hat beam. The rod has a diameter of 9.5 mm and a length of 20 mm. The heat transfer coefficient is obtained from a well-known equation suggested in [12] with water mass rate of 0.1 kg/s. The radius of the pumping beam is one-third of the outer rod radius where the fracture of this rod is seemed to occur at a pumping power of 93 W from each end where the tensile hoop stress reached 138 MPa. In this work, the hoop stress for the same pumping power is found to be equal to 143 MPa. Also, for the same case above the maximum temperature that could occur at the laser rod (predicted in ref. [2]) (at the centre of the pumped region) is 224°C while in this work, the result from the analytical solution is found to be equal to 218°C. These near by results may verify the accuracy of the mathematical model. The most probable reason for the small difference in results is that temperature-dependent thermal conductivity and thermal expansion coefficients were used in the numerical solution while in analytical solution fixed properties are used.

4. Result and discussion

A transient analytical solution for temperature distribution and hoop thermal stress using double-end-pumped laser rod is derived using the integral transform method. Analytical treatments possess several advantages over numerical solution: it reduces the computation time of the thermal effects, besides it is usually written in an explicit form so that one can indicate the effects of different parameters used in the solution. A double-end-pumped Nd:YAG rod has a length of 20 mm and a radius of 4.75 mm. Its facets are insulated while its lateral side is subjected to convection where the environmental temperature is 25°C. The pumping power is tested so as to induce hoop stress near the fracture limit. A simple code is written in Visual Basic 6 to implement the summation of eqs (6), (7), (9) after the roots of equation is obtained using Newton–Raphson method, and numerical integrations are carried out to obtain the values of Bessel's functions (J_0, J_1). The history of the maximum hoop stress for this rod having the aforementioned boundary conditions is shown in figure 2 (bold line). Without referring to a special crystal, factors that may affect the result are simply doubled to predict their effect on the induced maximum hoop stress.

Figure 2 shows the effect of different factors on the history of maximum hoop stress. It is clear that the increase in thermal conductivity reduces the maximum hoop stress: this is due to the decrease in temperature gradient which decreases the induced stress. Increasing heat transfer coefficient will induce more temperature gradients through the rod, which may increase stress, to some extent. Also the increase in heat factor increases the part of pumping power that converts to heat, which increases the induced stress. The increase in the expansion coefficient increases the induced strain and subsequently increases the induced stress. The increase in Poisson's ratio increases the transverse strain with respect to longitudinal strain, resulting in an increase in the transverse hoop and radial stresses. Increase in modulus of elasticity increases the tensile stress since more tensile stress yields for certain tensile strain as modulus of elasticity increases. The most effective factor that may influence maximum hoop stress is the absorption coefficient, since it is the reciprocal of the effective depth that absorbs power. Increasing absorption power within a small depth means high temperature gradient and consequently, high stress.

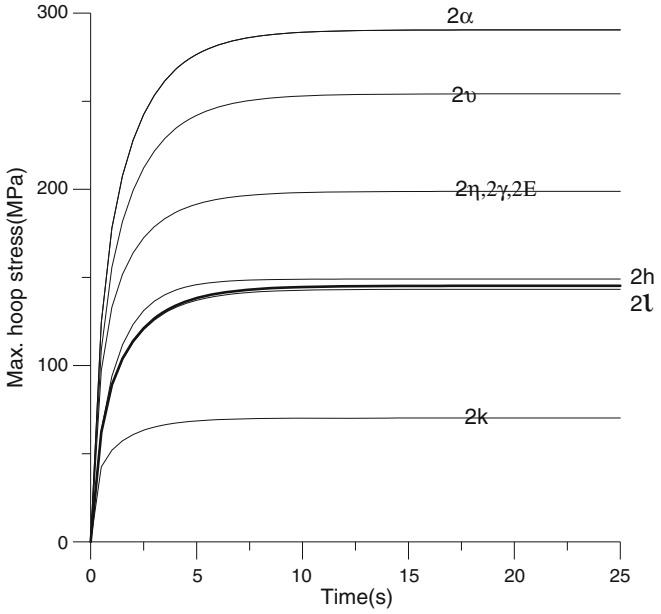

Figure 2. Maximum hoop stress history and influence of various factors on it.

From this figure, one can conclude that a crystal of high thermal conductivity, low heat factor, low Poisson's ratio, low expansion coefficient, low absorption coefficient and low modulus of elasticity extends the possible pumping power before failure occurs, but the length and convection heat transfer coefficient have a small effect on hoop stress and their variations are limited due to space and design considerations. Out of the four common types of crystals that are usually used in end pumping, we are looking for a crystal that has a high thermal conductivity, low absorption coefficient, low expansion coefficient, low heat factor and low product of $(M = \gamma E/(1 - \upsilon))$. Tm:YAP almost satisfies these conditions compared to the other crystals (see table 1).

Figure 3 shows the maximum temperature and hoop stress history for Nd:YAG and Tm:YAP. A significant reduction in maximum induced temperature and subsequent maximum hoop stress for the same pumping power (93 W from each end) is observed for

Table 1. Some optical, thermal and mechanical properties of laser crystals.

Crystal type	k (W/m·K)	α (1/m)	η (−)	$M \times 10^6$ (Pa/K)	$\rho c \times 10^6$ (J/m^3·K)
Nd:YAG [13]	10.3	350	0.32	3.631	1.82
Nd:GGG [12]	9	180	0.3	2.903	2.911
Tm:YLF (a-axis) [14]	7.2	143	0.33	1.455	3.081
Tm:YAP [15]	11	163	0.22	1.32	2.14

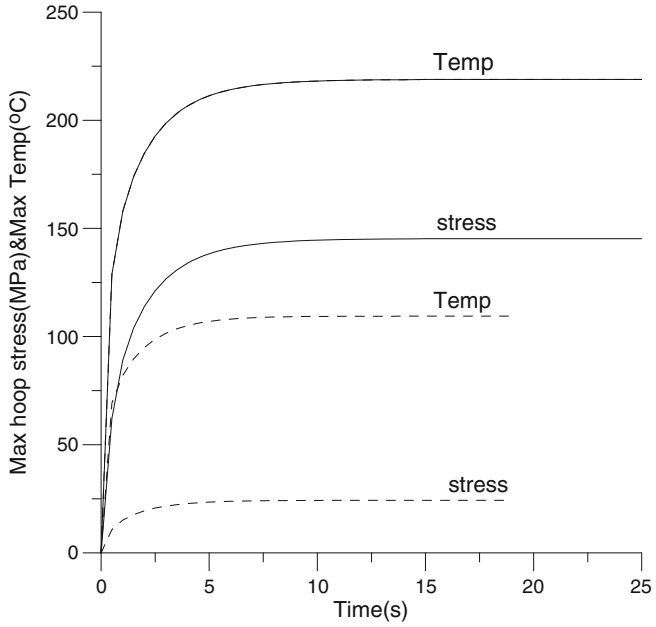

Figure 3. The maximum hoop stress and maximum temperature history. The solid line is for Nd:YAG and the dashed line is for Tm:YAP.

Tm:YAP crystal. This is due to the combined effects of various factors discussed above. In addition to that, a recent work shows that this crystal has higher overall efficiency [16] than an Nd:YAG crystal [13]. A final observation from figure 3 is that Tm:YAP

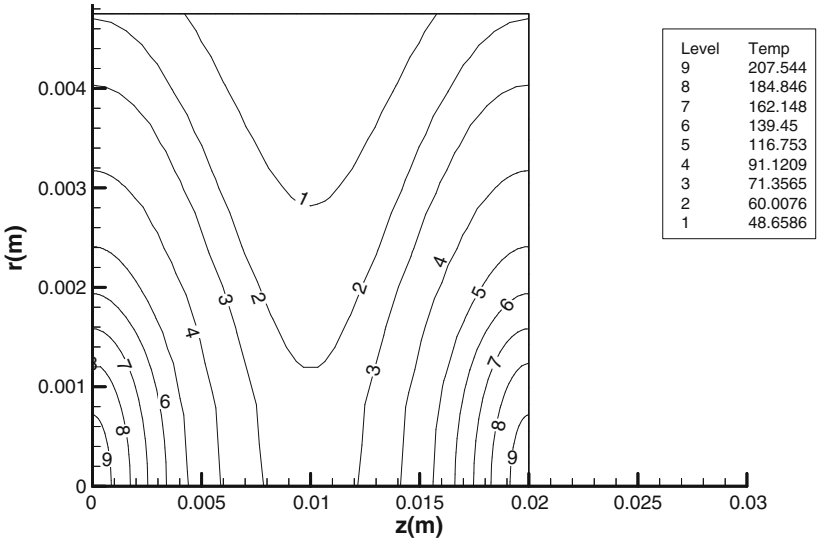

Figure 4. Steady-state temperature distribution in Nd:YAG laser rod (temp. is in °C).

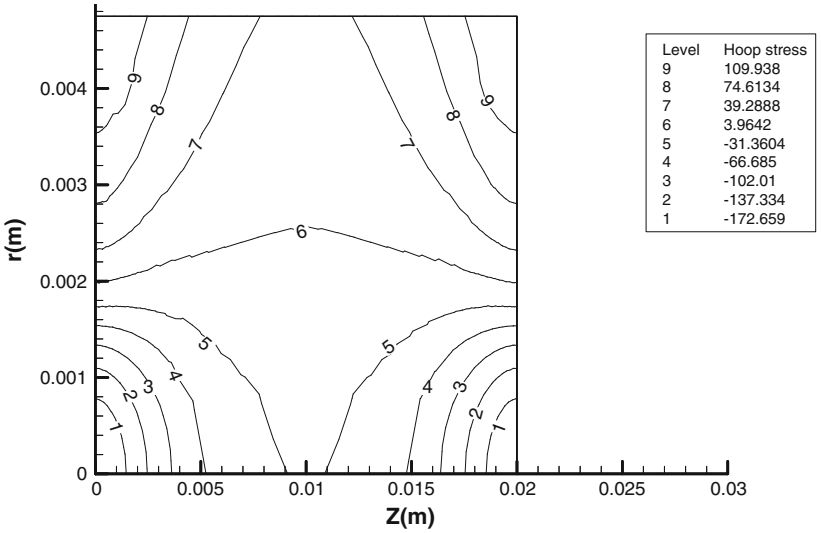

Figure 5. Steady-state stress distribution in Nd:YAG laser rod (stress in MPa).

can be brought to thermal equilibrium faster than an Nd:YAG. This is due to the reduction in thermal factor which produces less heat inside the laser rod. Laser rod having a small amount of heat takes less time to be brought to thermal equilibrium than a laser rod having higher heat, assuming same boundary conditions. Figures 4 and 5 show the temperature and hoop stress distributions in an Nd:YAG laser rod having aforementioned

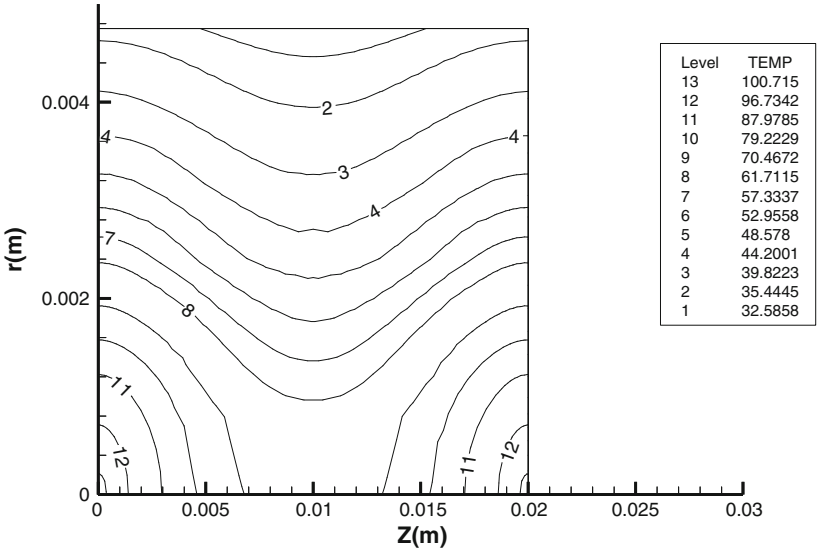

Figure 6. Steady-state temperature distribution in Tm:YAP laser rod (temp. in °C).

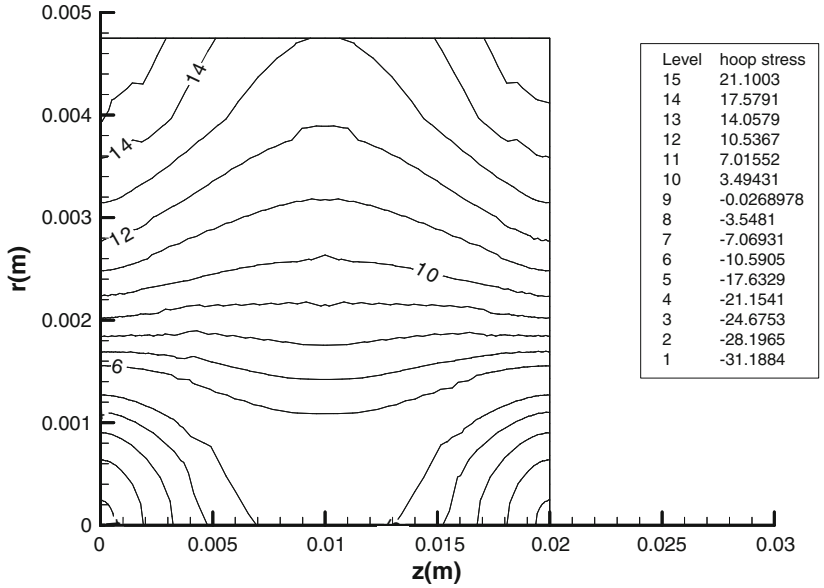

Figure 7. Steady-state stress distribution in Tm:YAP laser rod (stress in MPa).

boundary conditions. Figures 6 and 7 also show the temperature and hoop stress distributions but for Tm:YAP laser rod having the same aforementioned boundary conditions including pumping power of 93 W from each end. Note that the previous four figures show the upper half of the laser rod region and axes z and r are not to scale for each other. A clear reduction in temperature distribution is shown for Tm:YAP compared to that for Nd:YAG resulting in a significant reduction in induced hoop stress distribution assuming same pumping power and boundary conditions. This is due to the novel optical, thermal and mechanical properties of Tm:YAP crystal (see table 1).

It is well known that the origin of the thermal stress in the laser crystal is the induced temperature difference which is occurred due to the localized induced power and cooling requirements. In this work the maximum induced tensile stress for Tm:YAP is 25 MPa (see figure 3). Assume that the fracture limit of the Tm:YAP crystal is in the $\sim$160 MPa range [15] and wherever the tensile stress in the Tm:YAP rod exceeds this value (i.e. 160 MPa which is not the case in this work) there will be a permanent local modification in the crystal. Also the produced failure stress can happen at a pumping power much less than the power intensity that can produce shock waves.

5. Conclusions

The transient axis-symmetry heat equation for double-end-pumped laser rod has been solved analytically using integral transform method. The hoop stress, admitted to simulate failure through the rod, is derived also. The result of this work is compared with a well-verified finite element solution and a good agreement has been found. Some conclusions are drawn: to reduce hoop stress, one has to select a crystal that has high thermal

conductivity, low absorption coefficient, low thermal factor, low expansion coefficient and low product of $\gamma E/(1-\upsilon)$. Also it is found that beyond certain limits the heat transfer coefficient and rod length have insignificant effect on hoop stress. Tm:YAP almost matches these specifications where a significant reduction in thermal stress is observed compared to other types of crystals usually used in the end pumping method. Also, this crystal seems to have total efficiency more than Nd:YAG. It is also found that this crystal responds and reaches thermal equilibrium faster than the usual crystals used in the end pumping method.

References

[1] Y W Ma and Y Q Chen, *Laser devices* (Zhejiang University Press, Hangzhou, 1994)
[2] K S Shibib *et al*, *Thermal Sci*. **15**(Suppl. 2), S399 (2011)
[3] M P MacDonald, Th Graf, J E Balmer and H P Weber, *Opt. Commun*. **78**, 383 (2000)
[4] Th Graf, E Wyss, M Roth and H P Weber, *Opt. Commun*. **190**, 327 (2001)
[5] Ai-Yun Yao *et al*, *Chin. Phys. Lett*. **22(3)**, 607 (2005)
[6] Hamish Ogilvy, Michael J Withford, Peter Dekker and James A Piper, *Opt. Express* **11(19)**, 2411 (2003)
[7] M N Özisik, *Heat conduction* (Wiley, New York, 1980)
[8] Ananada K Cousins, *IEEE J. Quantum Electron*. **28**, 1057 (1992)
[9] Steve C Tidwell *et al*, *IEEE J. Quantum Electron*. **28**, 997 (1992)
[10] C Pfisther *et al*, *IEEE J. Quantum Elelectron*. **30**, 1605 (1994)
[11] Huseyin Yapici and Gamze Basturk, *J. Mater. Processing Technol*. **159**, 99 (2005)
[12] Feng Huang, Yuefeng Wang, Wenwu Jia and Wei Dong, *Proc. SPIE* **6823**, 682311 (2007)
[13] W Koechner, Solid-state laser engineering, in: *Springer Series in Opt. Sci*. (Springer, USA, 2006) 6th edn
[14] E H Bernhardil *et al*, *Optics Express*. **16**, 11115 (2008)
[15] Y Tian, G Li, B Q Yao and Y Z Wang, *Appl. Phys*. **B103**, 107 (2011)
[16] Xiaojin Cheng, Jianqiu Xu, Yin Hang, Guangjun Zhao and Shuaiyi Zhang, *Chin. Opt. Lett*. **9**, 091406 (2011)